




5-8-2017

# Inkjet Printing of Ag Nanoparticles using Dimatix Inkjet Printer, No 2

Ming Yuan Chuang

Follow this and additional works at: [http://repository.upenn.edu/scn\\_protocols](http://repository.upenn.edu/scn_protocols)

 Part of the [Biochemistry, Biophysics, and Structural Biology Commons](#), [Biomedical Engineering and Bioengineering Commons](#), [Chemical Engineering Commons](#), [Chemistry Commons](#), [Electrical and Computer Engineering Commons](#), [Engineering Science and Materials Commons](#), [Materials Science and Engineering Commons](#), and the [Physics Commons](#)

---

Chuang, Ming Yuan, "Inkjet Printing of Ag Nanoparticles using Dimatix Inkjet Printer, No 2", *Protocols and Reports*. Paper 40.  
[http://repository.upenn.edu/scn\\_protocols/40](http://repository.upenn.edu/scn_protocols/40)

This paper is posted at ScholarlyCommons. [http://repository.upenn.edu/scn\\_protocols/40](http://repository.upenn.edu/scn_protocols/40)  
For more information, please contact [repository@pobox.upenn.edu](mailto:repository@pobox.upenn.edu).

---

# Inkjet Printing of Ag Nanoparticles using Dimatix Inkjet Printer, No 2

## Abstract

This report describes the rheological analysis of the present Ag nanoparticle ink, and confirms that it is suitable for the piezoelectric drop-on-demand printing for both of 1 pL and 10 pL cartridges. The satellite drops and the splashing on the substrate are also discussed for optimization of the nozzle temperature and the jetting voltage. The minimum horizontal and vertical line widths are shown to be 30 and 40  $\mu\text{m}$ , respectively, but the average minimum single line width is estimated to be  $\sim 50 \mu\text{m}$ . The non-uniform width lines are suggested to arise from the bulge instability. Furthermore, it is indicated that the surface roughness of the PI film causes the non-parallel contact line pinning. The resistivity of printed lines is also reported.

## Keywords

Inkjet Printing, Ag nanoparticle, flexible printed electronics


## Disciplines

Biochemistry, Biophysics, and Structural Biology | Biomedical Engineering and Bioengineering | Chemical Engineering | Chemistry | Electrical and Computer Engineering | Engineering Science and Materials | Materials Science and Engineering | Physics

## Creative Commons License



This work is licensed under a [Creative Commons Attribution-Share Alike 4.0 License](https://creativecommons.org/licenses/by-sa/4.0/).

	Technical Report (Graduate Student Fellow Program)	Document No:
	Inkjet Printing of Ag Nanoparticles using Dimatix Inkjet Printer, No.2	Revision:
		Author: Ming-Yuan Chuang

## 1. Introduction

Inkjet printing has attracted a tremendous interest in printed flexible electronics, display, sensors, bio-arrays, solar cells, and ceramic component manufacture for the last decade.<sup>1,2,3,4</sup> Furthermore, the market of printed electronics is expected to exceed \$300 billion over the next 20 years.<sup>5</sup> Continuous, thermal drop-on-demand (DOD), and piezoelectric DOD inkjet printing technologies have been reported as the successful inkjet drop generation technologies so far, and especially piezoelectric DOD printing has been chosen for most applications in printing functional materials.<sup>4</sup> The piezoelectric DOD inkjet printer employs a piezoelectric element to drive current through the nozzles, ejecting droplets on the substrate according to the predefined digital design. DOD inkjet printing does not only provide a cost and time effective additive process for maskless micro-patterning, but also can digitally control the ejection of ink droplets of defined volume and print a pattern precisely at the desired location of the substrate. In addition, the inkjet printing is adaptable with Roll-to-Roll processing for manufacturing.

The goal of this project is to perform on-site inspection of piezoelectric DOD inkjet printer, Dimatix (DMP-2831, Fujifilm), at Quattrone Nanofabrication Facility (QNF), and to optimize the printing conditions on polyimide (PI) film. In the previous report, Abbas and Bajwa<sup>6</sup> demonstrated the successful printing of silver (Ag) nanoparticle ink on PI film using 10 pL ink cartridge, but found the inconsistency between the setup line width and print-out line width. The inconsistency countervails the advantage of controllability and efficiency for inkjet printing, and needs to be solved as the first priority.

This report describes the rheological analysis<sup>1,2,3,4,5,7,8</sup> of the present Ag nanoparticle ink, and confirms that it is suitable for the piezoelectric DOD printing for both of 1 pL and 10 pL cartridges. The satellite drops and the splashing on the substrate are also discussed for optimization of the nozzle temperature and the jetting voltage. The minimum horizontal and vertical line widths are shown to be 30 and 40  $\mu\text{m}$ , respectively, but the average minimum single line width is estimated to be  $\sim 50 \mu\text{m}$ . The non-uniform width lines are suggested to arise from the bulge instability. Furthermore, it is indicated that the surface roughness of the PI film causes the non-parallel contact line pinning. The resistivity of printed lines is also reported.

## 2. Experimental Section

### A. Materials

127  $\mu\text{m}$  thick polyimide (PI) films were purchased from McMaster-Carr. The 30-35 wt% Ag dispersion in triethylene glycol monomethyl ether was purchased from Sigma Aldrich, and had the following properties: Ag particle size  $\leq 50 \text{ nm}$ ; surface tension = 35-40 dyn/cm; viscosity = 10-18 cP; density =  $1.45 \pm 0.05 \text{ g/ml}$ ; resistivity = 11  $\mu\Omega\text{-cm}$ . The contact angle of the ink with PI film was previously reported to be  $10.6^\circ$ .<sup>6</sup>

### B. Measurement

The surface roughness and 3D profile of PI film were measured using Zygo New View 7300 optical profiler.

### C. Cartridge and Printing setup

1 pL and 10 pL ink cartridges were used in this study. Table 1 indicates the 1 pL and 10 pL cartridge specifications. Table 2 shows printing setups of 1 pL and 10 pL cartridges. The number of the active nozzles was set up to be one out of sixteen. After printing, the ink was sintered at  $150^\circ\text{C}$  for 30 min on a hot plate to remove the organic solvent and fuse Ag nanoparticles together to form conductive tracks.

Table 1. Cartridge Specification given by the manufacturer.

	Number of Nozzles	Nozzle Spacing	Nozzle Diameter	Calibrated Drop Volume	Maximum Jetting Frequency
<b>1 pL</b>	16	254 $\mu\text{m}$	<b>9 <math>\mu\text{m}</math></b>	1 pL	15 kHz
<b>10 pL</b>	16	254 $\mu\text{m}$	<b>21 <math>\mu\text{m}</math></b>	10 pL	60 kHz

Table 2. Printing setup for 1 pL and 10 pL cartridge.

	Substrate Temperature	Cartridge Temperature	Number of Active Nozzle	Jetting Voltage	Maximum Jetting Frequency	Meniscus Vacuum	Print Height
<b>1 pL</b>	50 $^{\circ}\text{C}$	<b>35 <math>^{\circ}\text{C}</math></b>	1	<b>20 V</b>	5 kHz	4.0 inchs- $\text{H}_2\text{O}$	0.400 mm
<b>10 pL</b>	50 $^{\circ}\text{C}$	<b>45 <math>^{\circ}\text{C}</math></b>	1	<b>40 V</b>	5 kHz	4.0 inchs- $\text{H}_2\text{O}$	0.400 mm

#### D. Drop Spacing

Resolution of inkjet printing can be adjusted from 5080 to 100 dpi by changing a cartridge mounting angle from 1.1 to 90  $^{\circ}$ , which results in increasing in drop spacing from 5 to 254  $\mu\text{m}$ . If the drop spacing is too short, the printed dots are overlapped too much, resulting in a large spread of the ink due to an outflow of the ink. In contrast, if the drop spacing is too long to overlap each other dot, a non-uniform width line or a separated dot is printed.<sup>2</sup> As discussed later, the drop spacings for 1 pL and 10 pL cartridges were set up to be 20 and 40  $\mu\text{m}$ , respectively, which were  $\sim 60\%$  of the diameters of the single dots, so that each dot was partially overlapped and coalesced adequately.

#### E. Waveform

The waveform controls the electrical signal driving the piezoelectric actuator on each nozzle. It has direct influence on the formation process of drop. Figure 1 shows a schematic diagram of waveform with five individual stages.

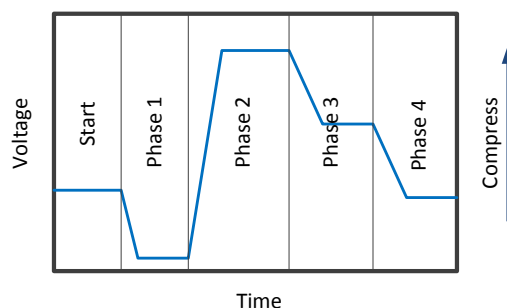


Figure 1. Schematic diagram of a typical waveform used in Dimatix inkjet printer.

1. Start, or stand by, the ink chamber is slightly compressed;
2. Phase 1, the voltage decreases that the piezoelectric element (PZT) moves upward and pulls ink into the chamber from the ink tank. It also pulls on the meniscus at the nozzle;
3. Phase 2, the chamber is compressed and eject a drop;
4. Phase 3, the voltage is brought back down to some bias level and control the breakup of leaving droplet and thinning filament (droplet tail from the nozzle).
5. Phase 4, the voltage goes back to stage 1 and prepare for the next ejection.

Figures 2 and 3 show the waveforms optimized for the present ink, and 1 pL and 10 pL cartridges. The voltage in phase 3 for 10 pL cartridge is increased a little when comparing with that for 1 pL cartridge, in order to tune the breakup process of the thinning filament.

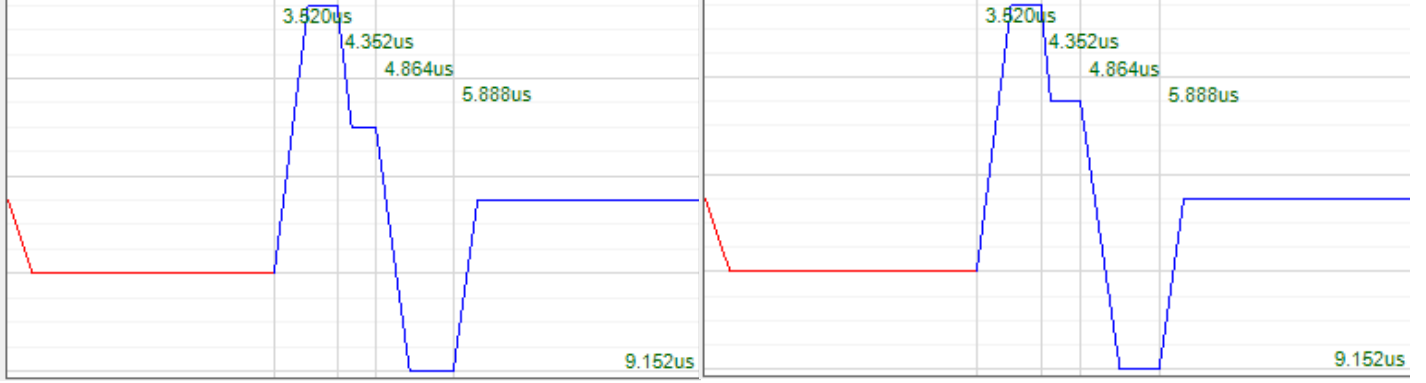


Figure 2. The waveform used for 1 pL cartridge

Figure 3. The waveform used for 10 pL cartridge

### 3. Results and Discussion

#### 3-1. Rheological parameters in inkjet printing

The fluid properties of the Ag nanoparticle ink will be discussed using the following rheological properties:<sup>2,4,8,9</sup>

$$Z = \frac{\sqrt{N_{We}}}{N_{Re}} = \frac{\eta}{\sqrt{\gamma\rho\alpha}} \quad (1)$$

where  $Z$  is the Ohnesorge number, which is described as a ratio between the Reynolds number ( $N_{Re}$ ) and the Weber number ( $N_{We}$ ). The Reynolds number is a dimensionless number, a ratio of inertial forces to viscous forces in fluid mechanics. The Weber number is a dimensionless number, a measure of the relative importance of the fluid's inertia compared to its surface tension.  $N_{Re}$  and  $N_{We}$  are given by the following equations:

$$N_{Re} = \frac{v\alpha\rho}{\eta} \quad (2)$$

$$N_{We} = \frac{v^2\alpha\rho}{\gamma} \quad (3)$$

where  $v$  is the velocity,  $\eta$  is the viscosity,  $\gamma$  is the surface tension,  $\rho$  is the density of the ink, and  $\alpha$  is the diameter of nozzle. The onset of splashing on drop impact is given by the following equation:

$$K = N_{We}^{1/2} N_{Re}^{1/4} \quad (4)$$

The splashing normally occurs when  $K$  exceeds the critical value ( $K_c$ ), although  $K_c$  depends on the substrate condition and temperature.<sup>10</sup> As shown above, the ink used in this study has the following fluid properties in SI units: viscosity,  $\eta = 10\text{-}18 \times 10^{-3} \text{ Pa}\cdot\text{s}$ ; surface tension,  $\gamma = 0.035\text{-}0.040 \text{ J/m}^2$ ; density,  $\rho = 1450 \text{ kg/m}^3$ . In addition, the diameters of the nozzles for 1 pL and 10 pL cartridges are  $9 \times 10^{-6}$  and  $2.1 \times 10^{-5} \text{ m}$ , respectively, and the contact angle of the ink on PI film is  $10.6^\circ$ .<sup>11</sup> The velocity,  $v$ , of the droplet in the inkjet printing can be estimated to be 6 m/sec, as discussed later. Table 3 indicates  $Z^{-1}$ ,  $N_{Re}$ ,  $N_{We}$ , and  $K$  estimated from Equations (1)-(4) for 1 pL and 10 pL cartridges.

Figure 4 shows a  $N_{Re}$ - $N_{We}$  plot of the 30-35 wt% Ag dispersion in this study, which is superimposed on the  $N_{Re}$ - $N_{We}$  plot of various fluids and suspensions reported in Ref. 9. The two parallel dotted lines for  $Z^{-1}$  indicate the  $1 < Z^{-1} < 10$

region suitable for the piezoelectric DOD printing. The three solid curves for  $\xi$  indicate various degrees of droplet spreading on impact.<sup>12</sup> The bold line of  $Kc = 100$  shows the onset of splashing ( $Kc = 100$  was given in Ref. 9, but  $Kc$  was modified to be 50 in Ref. 10). As can be seen in figure 4, the rheological parameters of  $Z$ ,  $N_{Re}$ ,  $N_{We}$ , and  $K$  for the 30-35 wt% Ag dispersion in this study is in the printable region.

Table 3. The inverse of the Ohnesorge number ( $Z^{-1}$ ), the Reynolds number ( $N_{Re}$ ), the Weber number ( $N_{We}$ ), and the splashing parameter ( $K$ ) estimated from Equations (1)-(4) for 1 pL and 10 pL cartridges.

	$Z^{-1}$	$N_{Re}$	$N_{We}$	$K$
<b>1 pL</b>	1.2-2.3	4.4-7.8	11.7-13.4	4.9-6.1
<b>10 pL</b>	1.8-3.5	10.2-18.3	27.4-31.3	9.3-11.6

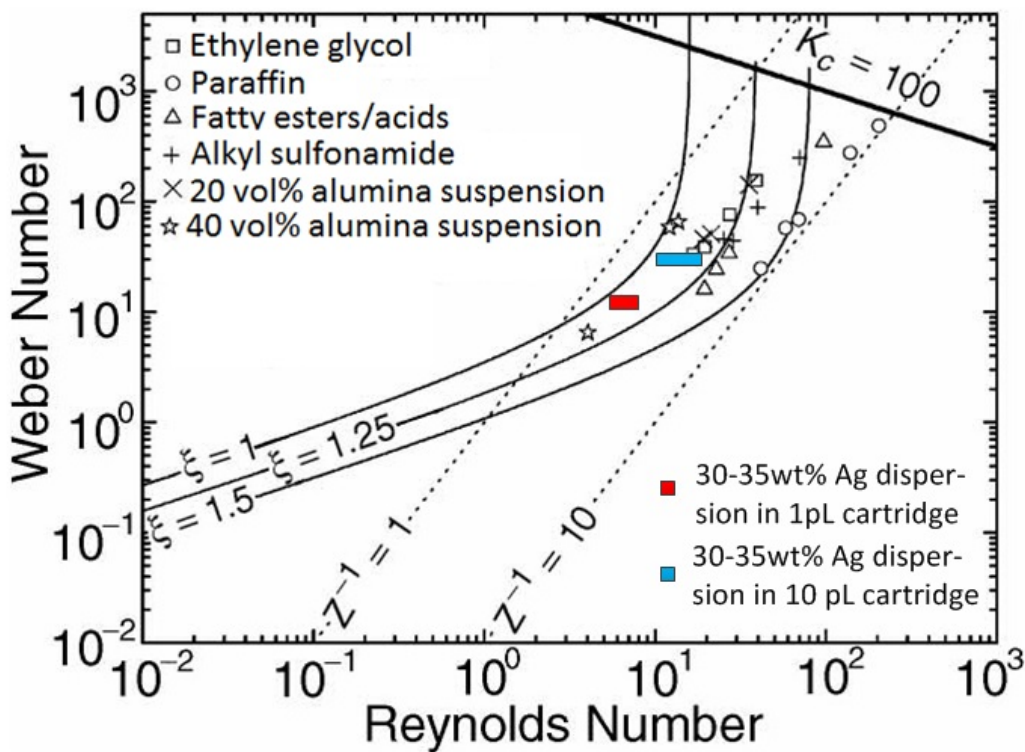


Figure 4. A  $N_{Re}$ - $N_{We}$  plot of the 30-35 wt% Ag dispersion used in this study, which is superimposed on the  $N_{Re}$ - $N_{We}$  plot of various fluids and suspensions with the relations of  $Z^{-1}$ ,  $\xi$ , and  $Kc$  in Ref. 9. The solid curves for  $\xi$  indicate contours of equal maximum droplet spreading.<sup>12</sup> The dotted lines for  $Z^{-1}$  indicate the boundaries of fluid properties typical of inkjet printers. The bold line for  $Kc = 100$  in the upper-right corner indicates the onset of splashing ( $Kc = 100$  was given in Ref. 9, but  $Kc$  was modified to be 50 in Ref. 10).

### 3-2. Nozzle temperature

The drop formation at the nozzle can be viewed as competition between viscous dissipation and surface tension. If  $Z^{-1} < 1$ , viscous dissipation is dominant in the drop formation, and prevents drop ejection from the nozzle. If  $1 < Z^{-1} < 10$ , the drop formation is stable. If  $Z^{-1} > 10$ , surface tension is dominant, forming droplets accompanied by unwanted satellite drops.<sup>2</sup> On the other hand,  $Z^{-1}$  increases with increasing in the nozzle temperature, due to combination of an exponential decay of the viscosity and a linear decay of the surface tension. Figure 5 shows CCD image of the drop formation at the nozzle temperatures of 43, 45, and 47 °C, using 10 pL cartridge. The satellite drop can be seen at the nozzle temperature of 47 °C in figure 5(c), whereas no satellite drop is observed at 43 and 45 °C.

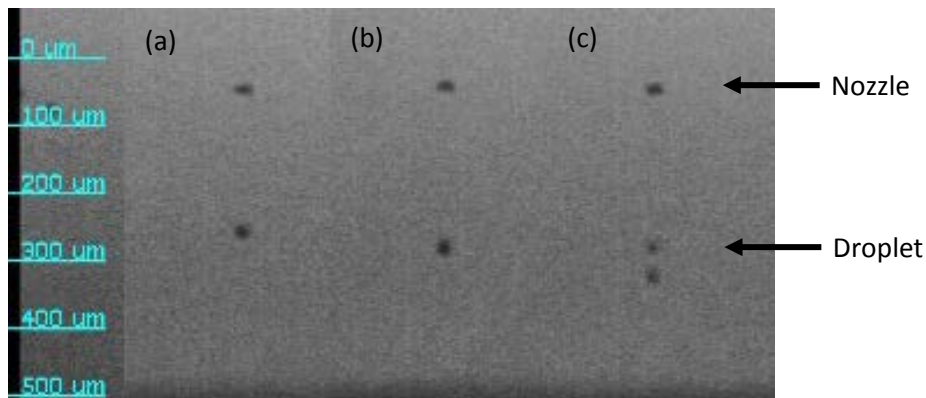


Figure 5. CCD Images of the drop formation for 10 pL cartridge at the nozzle temperature of (a) 43, (b) 45, and (c) 47 °C, captured by drop watcher 50  $\mu$ s after ejecting. In (c), the main drop is followed by a satellite drop at the nozzle temperature of 47 °C.

### 3-3. Jetting voltage

Figure 6 shows CCD images of jetting voltage dependence of the drop velocity, using 10 pL cartridge. The drop velocity is determined to be  $\sim$ 6m/sec at the jetting voltage of 37.5 V. It is noted that there is a minimum voltage required for the fluid to overcome the surface energy constrained by the orifice of nozzle.<sup>8</sup> As reported previously,<sup>6</sup> the minimum voltage for the present ink was determined to be 30 V for 10 pL cartridge. The printing stability increases with increasing in the drop velocity, due to decreasing in disturbance of the drop ejecting. However, if the drop velocity is too high, a splashing of the ink will occur when the drops land on the substrate. As indicated above, the nozzle temperature and jetting voltage need to be optimized for stabilizing and minimizing the drop formation and the printing.

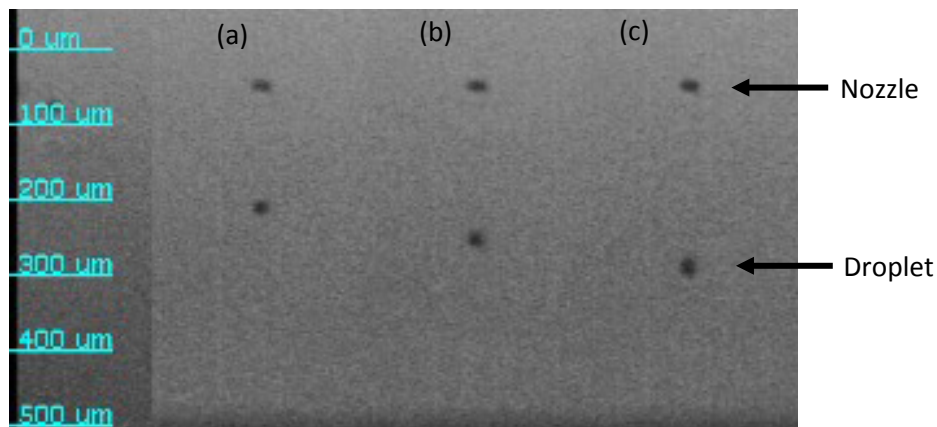


Figure 6. CCD Images of drop formation at the jetting voltage of (a) 35, (b) 37.5, and (c) 40V, captured by drop watcher 50  $\mu$ s after ejecting. The distance of the drop traveling for 50  $\mu$ s after ejecting increases with increasing in the jetting voltage, indicating that the drop velocity depends on the jetting voltage. The drop velocity is  $\sim$ 6m/sec at the jetting voltage of 37.5 V.

### 3-4. Separated dots array

Figure 7 shows optical microscope images of dot arrays for (a) 1 pL and (b) 10 pL cartridges. The average dot diameters for 1 pL and 10 pL cartridges are  $34.2 \pm 1.9$  and  $65.4 \pm 3.2$   $\mu\text{m}$ , respectively. It is important to determine the dot size to decide the drop spacing for printing continuous lines and patterns. The manufacturer suggests that the drop spacing should be set to be 50% of the dot diameter. In this study, however, the drop spacings for 1 pL and 10 pL cartridges were set up to be 20 and 40  $\mu\text{m}$ , respectively, which were 58 and 61 % of the dot diameters, respectively, because of the surface tension of the ink. It is noted that the coffee stain effect<sup>13</sup> also occurs when the solvent vaporizes.

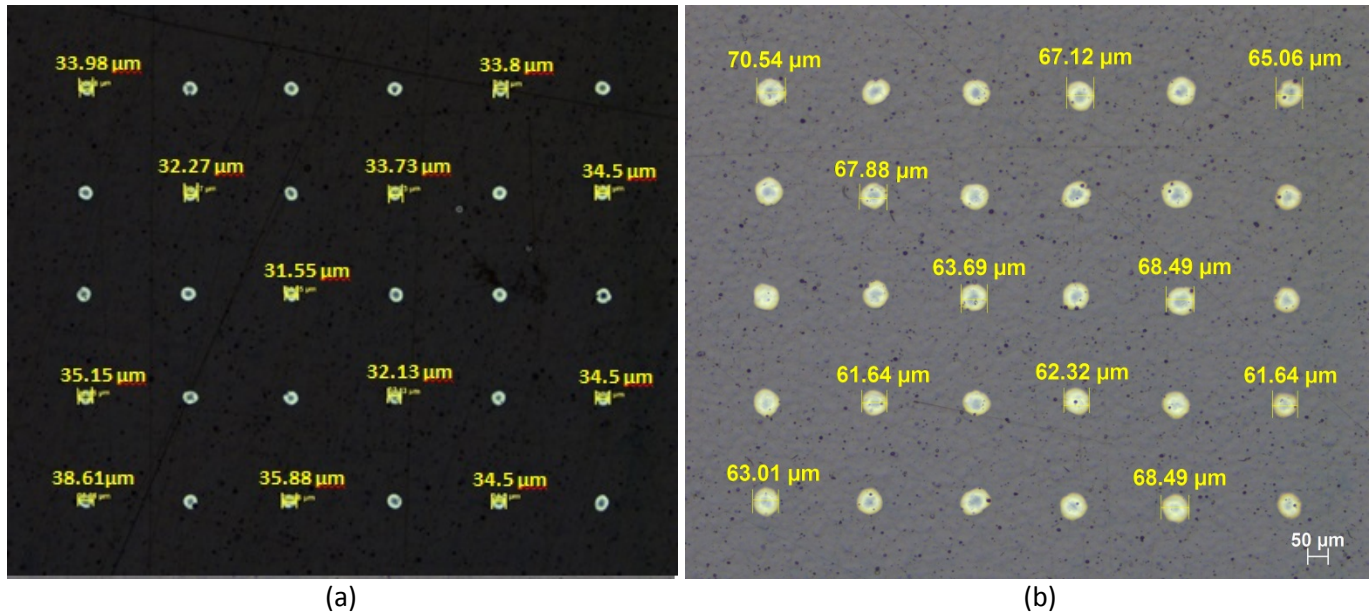
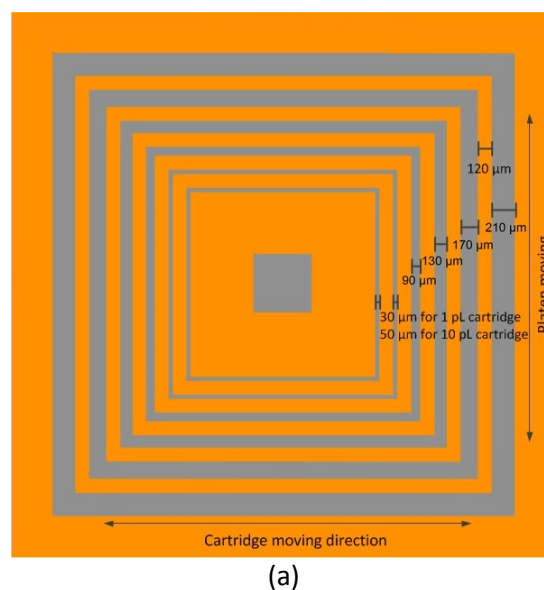


Figure 7. Optical microscope images of dots array for (a) 1 pL and (b) 10pL cartridge. The average dot diameters for 1 pL and 10 pL cartridges are  $34.2 \pm 1.9$  and  $65.4 \pm 3.2$   $\mu\text{m}$ , respectively. Both of them show the coffee stain effect.

### 3.5. Printing

Figure 8 shows (a) illustration of the printing pattern, and optical microscope images of the inkjet printing using (b) 1 pL and (c) 10 pL cartridge. The inner two square lines are single dot ones to show the minimum feature width of each cartridge.





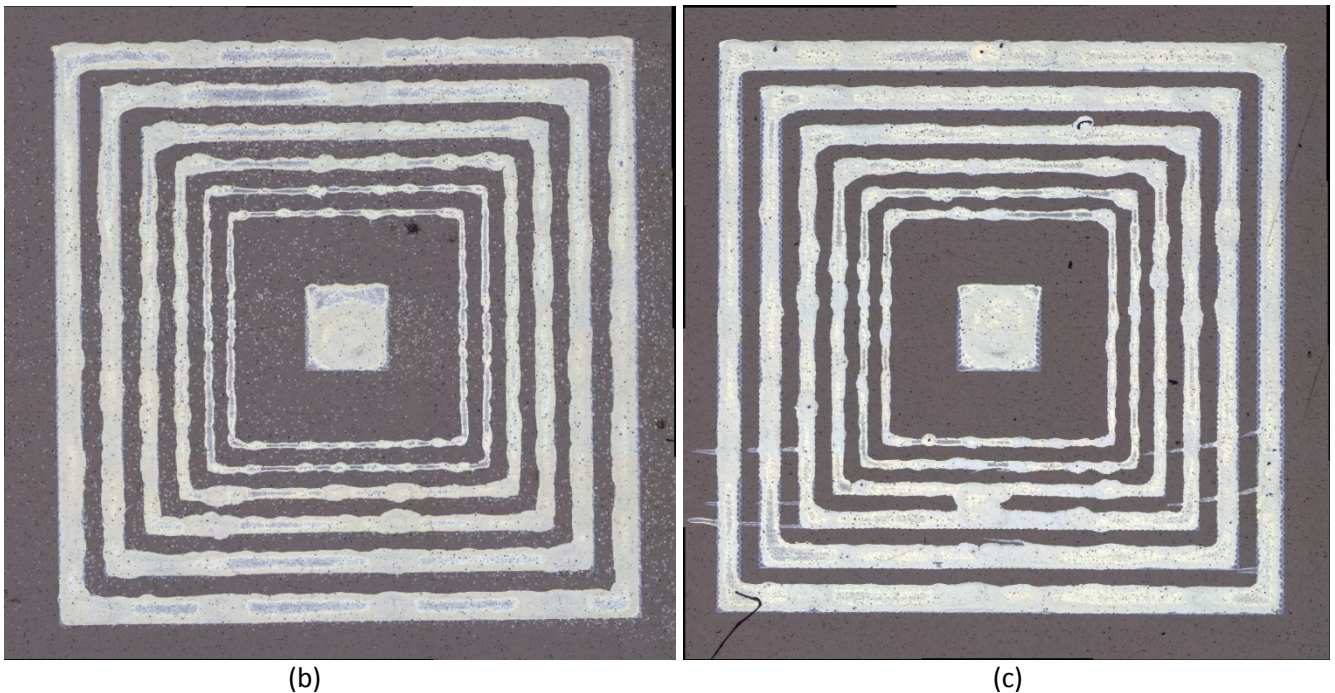


Figure 8. (a) Illustration of the printing pattern, and optical microscope images of the inkjet printing using (b) 1 pL and (c) 10 pL cartridge. In (a), the orange area shows the PI film substrate and the grey area indicates the silver pattern. The inner two square lines are set to be a single dot line to show the minimum feature width. The interval distances are 120  $\mu\text{m}$ .

Figures 9 and 10 show optical microscope images of the horizontal and vertical lines of the inkjet printing using 1 pL and 10 pL cartridges, respectively, indicating that the minimum horizontal line widths for 1 pL and 10 pL cartridges are 30 and 48  $\mu\text{m}$ , respectively, whereas the minimum vertical line widths for 1 pL and 10 pL cartridges are 40 and 54  $\mu\text{m}$ , respectively. However, the average minimum single line widths for 1 pL and 10 pL cartridges are estimated to be  $\sim 50$  and  $\sim 60$   $\mu\text{m}$ , respectively, and the root-mean-square (RMS) edge roughness is determined to be  $\sim 10$   $\mu\text{m}$ , using “ImageJ”.<sup>14</sup>

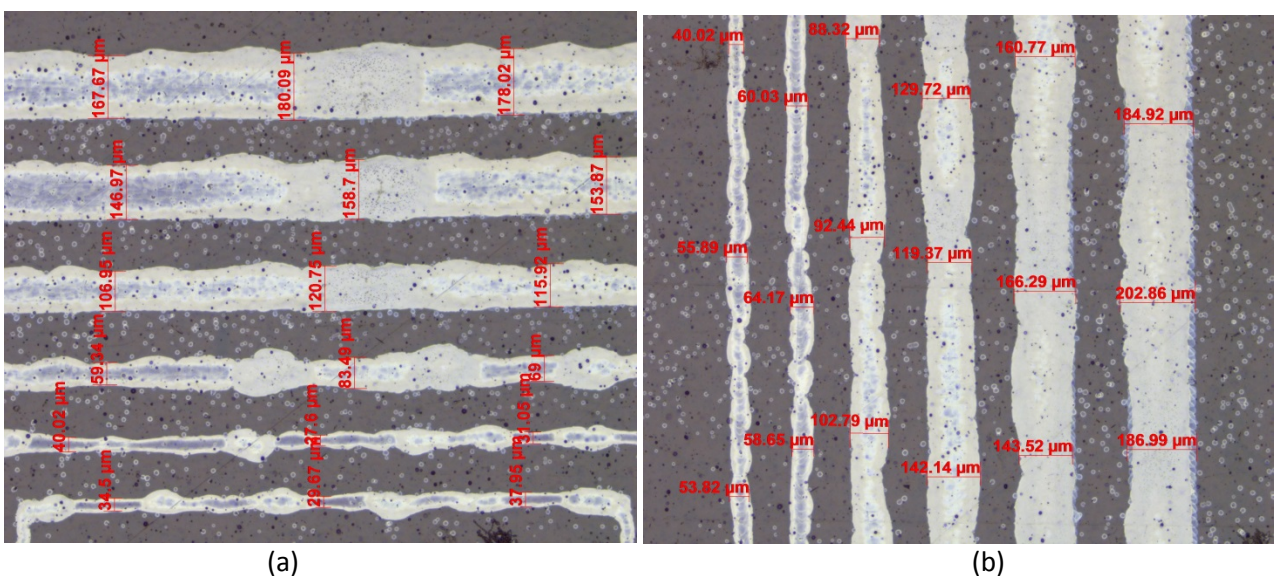


Figure 9. Optical microscope images of (a) the horizontal and (b) the vertical lines of the inkjet printing using 1 pL cartridge.

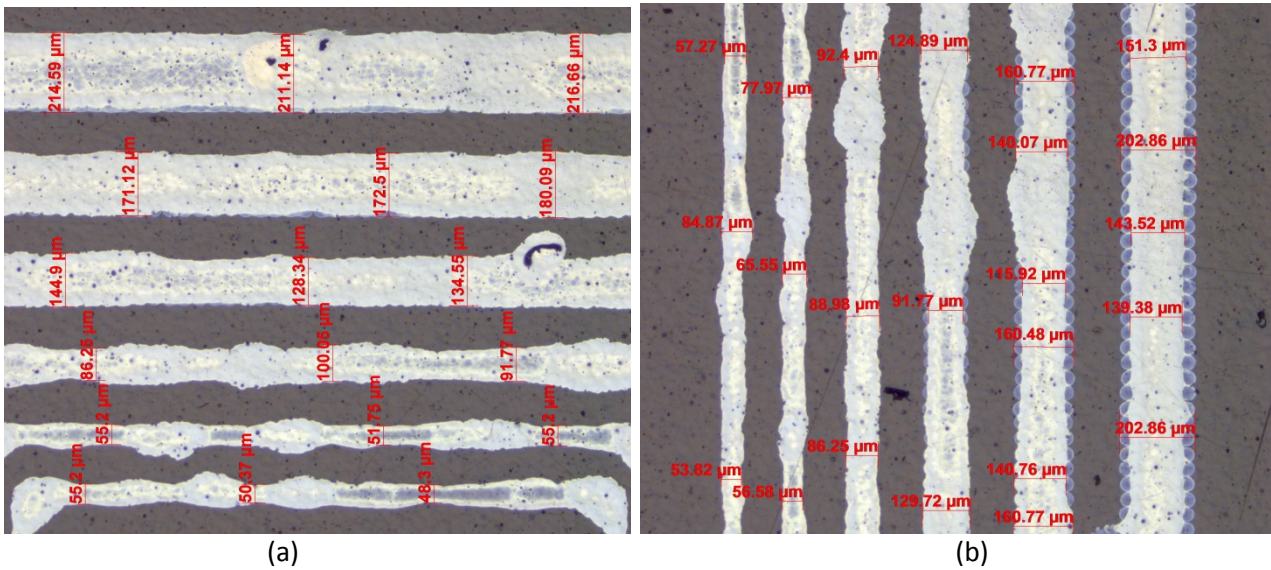


Figure 10. Optical microscope images of (a) the horizontal and (b) the vertical lines of the inkjet printing using 10 pL cartridge. In (b), it is noted that for the 210  $\mu\text{m}$  width set-up line, the outer line width with the semi-transparent dots is 203  $\mu\text{m}$ , whereas the inner line width without the dots is 139-151  $\mu\text{m}$ .

As can be seen in figures 9 and 10, the non-uniform width lines indicates the non-parallel contact line pinning.<sup>5</sup> Derby pointed out that bulge instability develops when the drop spacing is below the threshold determined by both of the contact angle and printing speed.<sup>4</sup> It is also suggested that the non-parallel contact line pinning is caused by a non-parallel side line of the Ag dispersion due to the roughness of the present PI film. Figure 11 shows (a) optical microscope zoom-in image of the 50  $\mu\text{m}$  width line printed on the PI film and (b) 3D optical surface profile of the blank PI film. Figure 11(a) reveals that the line edge is pinned and dragged by the scratch. Figure 11(b) exhibits  $\sim 800$  nm height protrusions, which should affect the contact line of the Ag dispersion, although the RMS surface roughness is 46 nm.

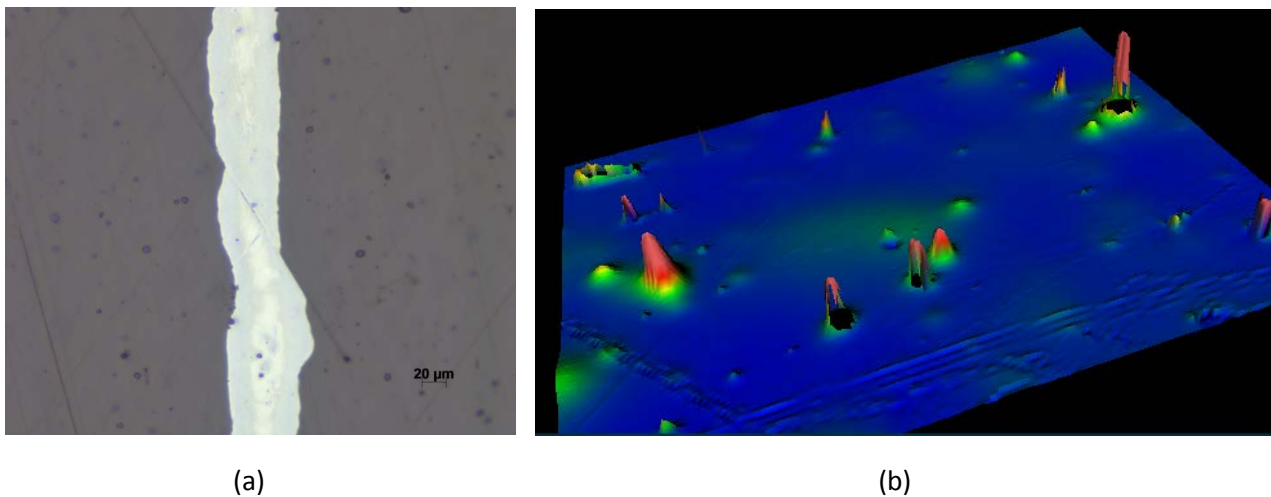


Figure 11. (a) Optical microscope zoom-in image of the 50  $\mu\text{m}$  width line printed on the PI film and (b) 3D surface profile of the blank PI film. In (b), the field of view is 140  $\mu\text{m}$  x 110  $\mu\text{m}$ , and the RMS surface roughness is 46 nm.

Figure 12 shows deviation of the average printed line widths from the set-up line widths for (a) 1 pL and (b) 10 pL cartridges. Figure 12(a) for 1 pL cartridge indicates that the deviation of the 90 to 210  $\mu\text{m}$  width horizontal and vertical lines is less than 10 %, confirming that the printing is controllable very well. However, the deviation of the 30  $\mu\text{m}$  width line is estimated to be 61-83 % due to the edge roughness, as discussed above. On the other hand, figure 12(b) for 10 pL cartridge exhibits that the deviation of the 90 to 210  $\mu\text{m}$  width horizontal lines is less than 10

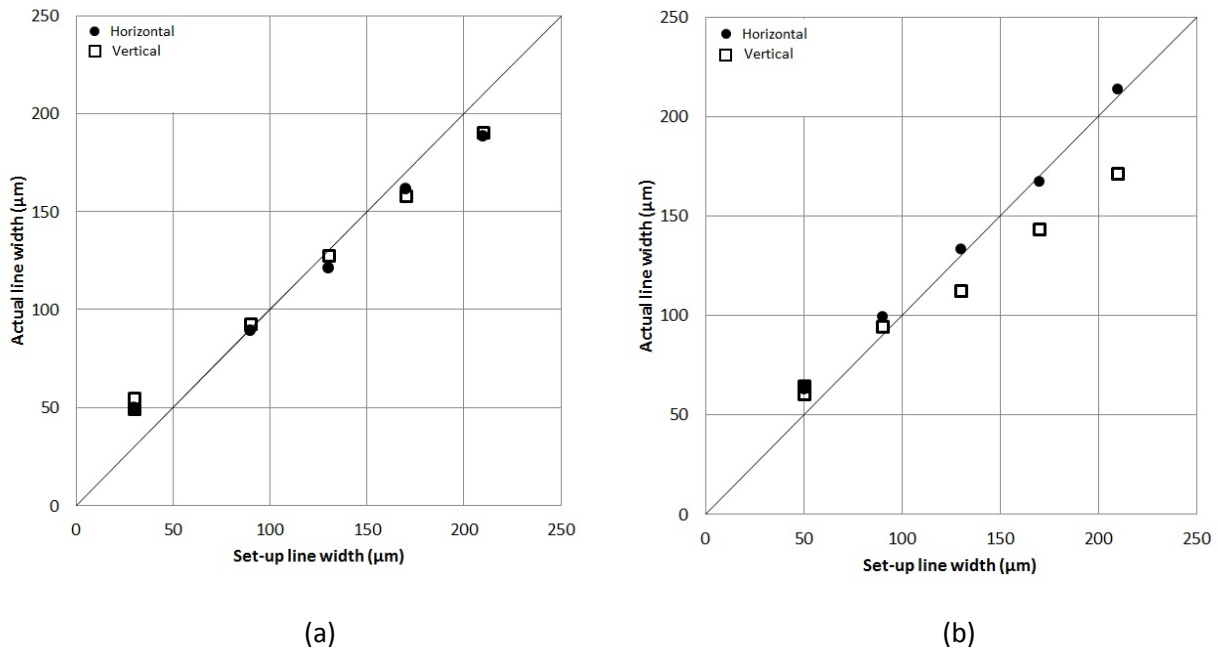


Figure 11. Deviation of the average printed line widths from the set-up line widths for (a) 1pL and (b) 10 pL cartridges. If the actual printed line width is the same as the set-up width, it should be on the solid line.

%, whereas the one of the 130 to 210 μm width vertical lines is 14-18 %. The edges of the vertical lines in figure 10 (b) reveal semi-transparent non-overlapped dots, implying that the actual drop spacing in the vertical line is deviated from that in the horizontal line. Since “ImageJ” counts the edge roughness of the semi-transparent dots, the average line widths result in the deviation of 14-18%. The cause of the semi-transparent dots is unknown.

### 3-6. Resistivity

The resistivity of printed lines is  $2.3 \times 10^{-6} \Omega\cdot\text{cm}$  measured by the two-point probe method using the following equation:

$$\rho = \frac{AR}{l} \quad (6)$$

where  $\rho$  is the resistivity,  $R$  is the resistance,  $A$  is the cross section of the line, and  $l$  is the length. The resistivity of  $2.3 \times 10^{-6} \Omega\cdot\text{cm}$  is larger by 44 % than the resistivity of bulk Ag =  $1.6 \times 10^{-6} \Omega\cdot\text{cm}$ , but 21 % of the original ink resistivity of  $1.1 \times 10^{-5} \Omega\cdot\text{cm}$ . The decrease in the resistivity from the ink to the printed line is ascribed to coalesce of Ag nanoparticles by sintering the ink.

## 4. Summary

The rheological analysis has confirmed that the present Ag nanoparticle ink is suitable for the piezoelectric DOD printing for both of 1 pL and 10 pL cartridges, indicating that the inverse of the Ohnesorge number,  $Z^{-1}$ , is in the range of  $1 < Z^{-1} < 10$ . The nozzle temperatures for 1 pL and 10 pL cartridges were optimized to be 35 and 45 °C, respectively, in order not to cause the satellite drops. The jetting voltages for 1 pL and 10 pL cartridges were determined to 20 and 40 V, respectively, in order to stabilize the drop ejecting, but not to splash the ink upon the substrate. The average dot diameters for 1 pL and 10 pL cartridges were  $34.2 \pm 1.9$  and  $65.4 \pm 3.2 \mu\text{m}$ , respectively, from which the drop spacings for 1 pL and 10 pL cartridges were set up to be 20 and 40 μm, respectively. The minimum horizontal line widths for 1 pL and 10 pL cartridges were 30 and 48 μm, respectively, whereas the

minimum vertical line widths for 1 pL and 10 pL cartridges were 40 and 54  $\mu\text{m}$ , respectively. However, the average minimum single line widths for 1 pL and 10 pL cartridges were estimated to be  $\sim 50$  and  $\sim 60$   $\mu\text{m}$ , respectively. The RMS edge roughness was determined to be  $\sim 10$   $\mu\text{m}$ , which directly affected the deviation of the thin lines from the set-up widths. The non-uniform width lines arose from the non-parallel contact line pinning, suggesting the bulge instability. Furthermore, it was also indicated that the surface roughness of the PI film caused the non-parallel contact line pinning. The resistivity of printed lines was determined to be  $2.3 \times 10^{-6}$   $\Omega\text{-cm}$  by the two-point probe method.

## References

- <sup>1</sup> A. Kamyshny and S. Magdassi, "Conductive Nanomaterials for Printed Electronics", *small* **10**, 3515 (2014).
- <sup>2</sup> J. Alamán, R. Alicante, J.I. Peña and C. Sánchez-Somolinos, "Inkjet Printing of Functional Materials for Optical and Photonic Applications", *Materials* **9**, 910 (2016).
- <sup>3</sup> B. Derby, "Printing and Prototyping of Tissues and Scaffolds", *SCIENCE* **338**, 921 (2012).
- <sup>4</sup> B. Derby, "Inkjet printing ceramics: From drops to solid", *J. Eur. Cera. Soc.* **31**, 2543 (2011).
- <sup>5</sup> M. Singh, H. M. Haverinen, P. Dhagat, G. E. Jabbour, "Inkjet Printing-Process and Its Applications" *Adv. Mater.* **22**, 673 (2010).
- <sup>6</sup> A. Abbas and I. Bajwa, "Inkjet Printing of Ag Nanoparticles using Dimatix Inkjet Printer, No.1", [http://repository.upenn.edu/scn\\_protocols/37/](http://repository.upenn.edu/scn_protocols/37/), (2017).
- <sup>7</sup> N. Reis and B. Derby, "Ink jet deposition of ceramic suspensions: modelling and experiments of droplet Formation", *MRS Proc.* **625**, 117 (2000).
- <sup>8</sup> P.C. Duineveld, M.M. de Kok, M. Buechel, A. Sempel, K.A. Mutsaers, P. van de Weijer, I.G. Camps, T. van de Biggelaar, J.-E.F. Rubingh, E.I. Haskal, "Ink-jet printing of polymer light-emitting devices", *SPEI Proc.* **4464**, 59–67 (2002).
- <sup>9</sup> B. Derby and N. Reis, "Inkjet Printing of Highly Loaded Particulate Suspensions", *MRS BULLETIN*, **28**, 815 (2003).
- <sup>10</sup> B. Derby, "Inkjet Printing of Functional and Structural Materials: Fluid Property Requirements, Feature Stability, and Resolution", *Annu. Rev. Mater. Res.* **40**, 395–414 (2010).
- <sup>11</sup> The contact angle is important for the drop spreading on impact on the substrate. See Ref. 12.
- <sup>12</sup> (a) M. Pasandideh-Fard, Y.M. Qiao, S. Chandra, and J. Mostaghimi, *Phys. Fluids* **8**, 650 (1996). The authors have modeled the spreading process of the droplet on impact on the substrate:

$$\xi = \frac{d_{max}}{d} = \left( \frac{N_{We} + 12}{3(1 - \cos \theta_{eq}) + 4(N_{We}/N_{Re}^{1/2})} \right)^{1/2} \quad (i)$$

where  $d_{max}$  is the maximum diameter of spreading,  $d$  is the radius of the impinging droplet and  $\theta_{eq}$  the equilibrium contact angle.  $\xi$  of the present Ag dispersion on PI film is determined to be 1.0-1.2.; (b) D. B. Van Dam and C. Le Clerc, "Experimental study of the impact of an ink-jet printed droplet on a solid substrate", *Phys. Fluids* **16**, 3403 (2004). On the other hand, the equilibrium contact diameter of the drop,  $d_{eq}$ , is also given by the following equation:

$$\beta = \frac{d_{eq}}{d} = \left( \frac{8}{\tan \frac{\theta_{eq}}{2} \left( 3 + \left( \tan \frac{\theta_{eq}}{2} \right)^2 \right)} \right)^{1/3} \quad (ii)$$

$\beta$  of the present Ag dispersion on PI film is determined to be 3.1-3.2.

<sup>13</sup> Coffee stain effect: At low contact angles, the fluid close to the contact line is adjacent to a large dry surface, and this enhances evaporation of the solvent, leading to a ring of particles coming out of suspension or dispersion. Furthermore, the presence of this dried deposit pins the contact line and prevents it from retracting. This contact line pinning results in the receding contact angle decreasing as solvent is removed, and the flow of particles to the contact line ends up with particle segregation and a ring deposit.

<sup>14</sup> Justin R. Bickford, "Analyze\_Stripes, Script for ImageJ" [http://imagejdocu.tudor.lu/doku.php?id=macro:analyze\\_stripes](http://imagejdocu.tudor.lu/doku.php?id=macro:analyze_stripes)